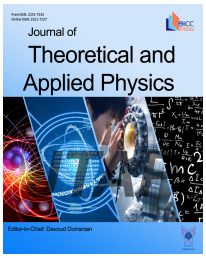

Volume 18, Issue 4, 182447 (1-11)

Journal of Theoretical and Applied Physics (JTAP)

https://dx.doi.org/10.57647/j.jtap.2024.1804.47

Enhancing cell growth with PAN/PVA-gelatin 3D scaffold using in-situ UV radiation electrospinning and plasma treatment

Rahimeh Khavari[1], Saeed Javadi Anaghizi[2], Ahmad Khademi[2], Mehdi Jahanfar[1,*], Shirin Farivar[1,*], Hamid Ghomi[2]

[1]*Department of Cell & Molecular Biology, Faculty of Life Sciences & Biotechnology, Shahid Beheshti University, Tehran, Iran.*
[2]*Laser and Plasma Research Institute, Shahid Beheshti University, Tehran, Iran.*

[*]**Corresponding author:** jahanfarmehdi170@gmail.com, s_farivar@sbu.ac.ir

Original Research

Received:
9 April 2024
Revised:
20 May 2024
Accepted:
1 June 2024
Published online:
30 August 2024

Abstract:

The hydrophobic nature of synthetic polymers poses a substantial barrier since it limits cell-seeding and proliferation scaffold performance. To overcome this challenge, the present research attempts to employ in-situ UV electrospinning and plasma surface modification techniques to fabricate a three-dimensional PAN/PVA-gelatin scaffold. The proposed scaffold holds great potential in mitigating hydrophobicity limitations, thereby facilitating enhanced cell adhesion and proliferation. The SEM results indicated that exposure to UV irradiation resulted in the formation of wavy shapes in the PAN microstructures and crosslinking between fibers within the scaffold. Moreover, plasma treatment induced the formation of pores on the PAN surface, with an average diameter of 43 μm, corresponding to the size range of mouse fibroblast cells. Furthermore, the plasma treatment provided roughness augmentation of the scaffold surface, which played a crucial role in enhancing cell adhesion and elongation on the modified scaffold surface. Comparatively, the plasma-modified scaffolds exhibited a higher proportion of viable cells than the unmodified scaffolds ($p < 0.05$). Moreover, the implementation of perforations in the PAN layer via plasma treatment reduced the number of necrosis cells in comparison to the other samples. In contrast, the unmodified scaffold showed a higher percentage of apoptosis cells ($p < 0.05$).

Keywords: Three-dimensional scaffolds; In-situ UV electrospinning; Plasma treatment; Fibroblast cells; Tissue engineering

1. Introduction

Polymer scaffolds are increasingly prevalent in tissue engineering (TE) and regenerative medicine owing to their ability to offer a three-dimensional structure that supports cell proliferation and differentiation, and can be fabricated to mimic the extracellular matrix of multiple tissues [1–4]. Fabrication techniques for polymer scaffolds include self-assembly, phase separation, and electrospinning [5–8]. Electrospinning is a highly versatile, cost-effective, and sustainable method for manufacturing scaffolds using a diverse range of polymer materials [9, 10]. The process employs electrostatic forces to produce uniform fibers, yielding structures that demonstrate a noteworthy degree of precision and uniformity [11]. Biodegradable polymers such as polycaprolactone (PCL), poly-lactic acid (PLA), poly-trimethyl ethylene carbonate (PTMC), and poly-glycolic acid (PGA) have gained significant attention in the TE field [12]. The surface properties of scaffolds have a notable impact on biological properties, including but not limited to cell adhesion, proliferation, and differentiation. Throughout the past few decades, cold plasma treatment has emerged as an advanced technique for surface modification [13].

The cold plasma (CP) treatment is a non-thermal, non-chemical, and eco-friendly approach to modifying polymer surfaces without affecting bulk characteristics [14]. It allows for the modification of surface chemistry, topography,

and morphology of polymer scaffolds. These modifications can enhance the scaffold's wettability, surface energy, and surface roughness [15], which in turn facilitate cell adhesion, proliferation, and differentiation. The CP treatment has been observed to improve the biological properties of polymer scaffolds by enhancing the attachment and growth of mesenchymal stem cells (MSCs) and promoting their differentiation into osteoblasts, chondrocytes, and adipocytes [16]. Furthermore, this technique has the potential to enhance the biocompatibility of polymer scaffolds by mitigating of the inflammatory response of host tissues [17, 18].

In the 1990s, scientists began investigating plasma surface treatments as a means of modifying polymer surface properties for biomedical applications. One of the earliest studies on the effects of plasma treatment on polymer scaffolds was conducted by Nitschke, Mirko, et al. in 2002 [19]. They examined how plasma treatment altered the surface properties and surface-selective chemical activation of poly (3-hydroxybutyrate) (PHB) scaffolds. Plasma treatment effectively converted the hydrophobic properties of PHB to hydrophilic while preserving the morphology of the scaffold. Since then, numerous studies have been conducted on the plasma surface modification of polymer scaffolds using various polymers such as poly-lactic-co-glycolic acid (PLGA) [20, 21], poly (ε-caprolactone) (PCL) [22, 23], polyethylene glycol (PEG) [24], and polyurethane (PU) [25, 26]. These studies collectively highlight the potential of plasma treatment to modify the surface properties of polymer scaffolds for tissue engineering purposes.

The objective of this investigation is to assess the influence of plasma treatment on the attachment and survival of fibroblast cells. The study focuses on the impact of surface modification and variation on the polymer surface. A three-dimensional scaffold was fabricated using the electrospinning technique, employing polyacrylonitrile (PAN) and polyvinyl alcohol-gelatin (PVAG) polymers. Ultraviolet light exposure was applied simultaneously to enhance the structural stability of the scaffold. To evaluate the viability and proliferation of fibroblast cells, a comprehensive investigation employing flow cytometry and scanning electron microscopy (SEM) imaging was performed. Furthermore, the examination of surface topography was conducted using both SEM and atomic force microscopy (AFM), allowing for a comprehensive analysis of the cellular structure.

2. Materials and methods

2.1 Materials

The polymeric materials employed in this research were carefully selected for their unique properties. The PVA (Mw = 120 kg/mol), PAN (Mw = 80 kg/mol), gelatin, and dimethyl-formamide (DMF), which was utilized as a solvent for the polymeric solution, were purchased from Merck Chemical Co. (USA). Malonic acid (MA) and glacial acetic acid were obtained from Sigma-Aldrich (St. Louis, MO, USA). Fetal bovine serum (FBS), high-glucose Dulbecco's modified Eagle medium (DMEM), antibiotics (penicillin and streptomycin), trypsin, and phosphate-buffered saline (PBS, pH = 7.4) were acquired from Thermo-Fisher Scientific under the Gibco brand. The selection of materials and reagents was based on their quality and reliability to ensure precise and consistent outcomes.

2.2 Preparation of polymer solutions

The polymer scaffold was reinforced by applying a PAN polymer and DMF solvent as the first layer. The PAN powder concentration of 15% w/v was dissolved in DMF and stirred on a magnetic stirrer at room temperature for two hours to ensure uniformity. The outer layer comprises PVA and gelatin polymers with MA and acetic acid solvents as chemical binding agents. A mixture of PVA (15% w/v) and gelatin (10% w/v) was prepared, with the addition of malonic acid (20% w/v of the total weight of PVA and gelatin), to produce the PVAG solution. The mixture was stirred on a magnetic stirrer at 50 °C for two hours, using acetic acid (80% v/v) as the solvent. The spinning solutions were subjected to ultrasonication for 30 minutes, loaded into a 3-mL syringe, and placed in a syringe pump after 24 hours of spinning. This step was taken to ensure the removal of any remaining bubbles.

2.3 Fabrication of nanofibrous scaffolds

The electrospinning process involved the utilization of an electrospinning machine at a voltage of 23 kV to transform the polymer solution into fibers. The polymer solution feeding rate was 1.2 mL/hour. The distance between the spinner head and the collector was 10 cm, while the drum rotation speed was set to 600 revolutions per minute (rpm). The fibers were woven, and to facilitate the in-situ cross-linking process with the electrospinning process, two Philips UV lamps with a power output of 10 watts each were positioned on the drum. The objective of this configuration served a dual purpose: to enhance the strength of the PAN layer and activate malonic acid as a cross-linker, while also facilitating gelatin molecules bonding within the PVAG layer. Fig. 1 depicts the schematic of the electrospinning setup.

2.4 Plasma surface treatment

There are two configurations of the dielectric barrier discharge (DBD) that are employed for direct and indirect plasma treatment of polymer surfaces. The DBD probes consist of a copper rod with a diameter of 10 mm, which

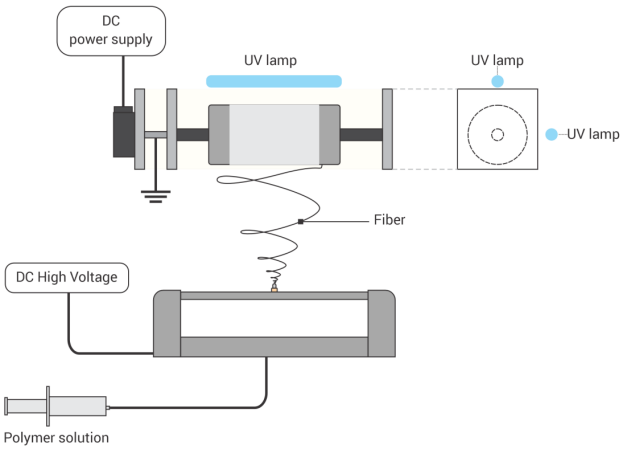

Figure 1. Schematic of electrospinning process.

serves as the high voltage (HV) electrode. The rod is insulated by a Teflon tube. To complete the probe assembly, a dielectric quartz plate with a thickness of 1 mm is added, along with a grounded aluminum mesh electrode. The primary distinction between direct and indirect plasma treatment lies in the presence or absence of the grounded aluminum mesh. In the direct configuration, this mesh is not present, whereas in the indirect configuration, it is included. The HV electrode is connected to a pulsed power supply that operates at a frequency of 6 kHz with a peak-to-peak voltage of 11.77 kV. The current and voltage applied to the HV electrode were recorded using a digital oscilloscope (TDS2024B Tektronix 200MHz), with a current probe (Tektronix TCP202) and a high-voltage probe (SEW PD-20S 1:1000). The detection of metastable plasma species was accomplished using the optical emission spectrometer (OES) model AvaSpec-ULS2048CL-EVO. Spectroscopy measurements were taken radially at 1 cm from the plasma. Fig. 2 illustrates the laboratory configuration of the DBD plasma in both direct and indirect modes, as well as the experimental setup utilized for acquiring the plasma diagnostic. The polymer fibers with dimensions of 1×1 cm dimensions are positioned 2 mm below the DBD probe and subjected to plasma treatment. To stabilize the cells on the scaffold, the PAN layer was treated with direct plasma for 10, 20, 35, 45, and 60 seconds. In contrast, the PVAG layer underwent indirect plasma for 3 minutes.

2.5 Fibroblast cell implantation

The mFib-2 cells, classified as "Normal" fibroblast-like cells, were isolated using the methodology outlined in prior research [27]. Then, they were cultured in a medium containing 78.5% DMEM high glucose, 10% FBS, and 1.5% antibiotics (penicillin and streptomycin) at 37 °C and 5% CO_2. Prior to placement in 12-well plates, the fibers underwent synthesis and plasma surface modification. The fibers were sterilized with 70% alcohol for 3 minutes, and then fibroblast cells were cultured on them. To evaluate cell viability and apoptosis, the cells were detached from the fiber surface and the plate after 48 hours of culture. This was achieved by treating the cells with trypsin enzyme for 5 minutes, gently tapping the plate multiple times, and transferring the cells to another culture medium. Subsequently, the cells were centrifuged for one minute, labeled, and prepared for Annexin-V-FITC flow cytometry analysis. The detached cells were centrifuged briefly and labeled with Annexin-V-FITC, a fluorescent dye that binds to phosphatidylserine exposed on the outer membrane of apoptotic cells. Additionally, propidium iodide (PI) was used as a counterstain to differentiate between early apoptotic and late apoptotic/necrotic cells. The labeled cells were then suspended in a buffer solution and analyzed using a flow cytometer. A biocompatibility assessment was performed on the upper surface of the scaffold. The selection of this specific region for evaluation was motivated by its regular and direct engagement with fibroblast cells. To assess the effectiveness of the fibers, a set of cellular experiments was conducted, encompassing three distinct conditions. These conditions consisted of a scaffold without plasma surface modification (UMS), as well as two plasma-modified scaffolds, one with and one without PAN layer treatment (PMSP and PMS, respectively). In order to assess the statistical significance of the observed disparities, a one-way analysis of variance (ANOVA) was conducted, followed by post-hoc analysis using Tukey's method to discern pairwise distinctions among the scaffolds.

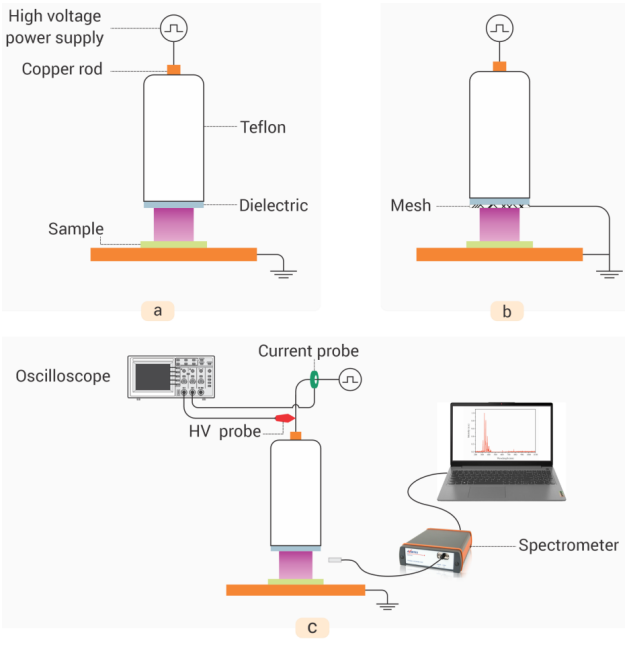

Figure 2. (a) Direct mode, (b) indirect mode of DBD plasma, and (c) diagnostic setup configuration.

2.6 Characterization

The SEM (Hitachi SU3500) was employed to investigate the surface morphology of fibers, both unmodified and plasma-modified. The fiber topography was investigated using AFM (NanoInk DPN500). The sessile drop technique was employed to conduct wettability evaluations, in which the apparent contact angle of distilled water droplets was determined. To ensure the precision and dependability of the data, three distinct samples were utilized for each condition during the measurement process. In order to conduct the experiment, a 10 mL volume of distilled water was carefully dispensed onto the surface of each individual sample. Then, a computer-linked camera was employed to capture and document images. The acquired images were subsequently analyzed using ImageJ software in order to ascertain the contact angles. Attenuated total reflectance Fourier transform infrared spectroscopy (ATR-FTIR) was utilized to analyze the surface chemical structure of the samples. The ATR-FTIR spectra were obtained with an ATR-FTIR-NEXUS 470 instrument from THERMO NICOLET CO, USA, in the wavenumber range of 4000 to 500 cm^{-1}, with 60 scans and a resolution of 4 cm^{-1}. flow cytometry technique was employed to assess the characteristics of the immune microenvironment of the scaffold. Following 48 hours of incubation of fibroblast cells cultured on the chip, the samples were stained with the Annexin-V-FITC kit.

3. Results and discussion

3.1 Discharge diagnosis

The current and voltage applied to the HV electrode is shown in Fig. 3 a. The average electrical power applied to the DBD probe is 5.58 W [28]. The plasma spectrum was obtained from DBD plasma that had been exposed to the surface of the scaffold, as shown in Fig. 3 b. This spectrum encompasses distinct spectral lines attributed to oxygen, nitrogen, and OH species [29]. The interaction between oxygen species and the polymer surface has the potential to initiate the formation of oxygen-based functional groups, leading to enhanced surface energy and improved hydrophilicity characteristics [30]. In addition, the presence of nitrogen species can facilitate the formation of nitrogen-containing functional groups, eventually enhancing polymer adhesion and promoting cell attachment [30, 31]. Furthermore, the dissociation of water vapor in plasma generates highly reactive OH radicals, which can readily react with the surface of polymer, leading to the introduction of hydroxyl groups. This process effectively heightens surface energy and improves wettability [30]. Prior studies have demonstrated that surface hydrophilicity and functional groups significantly impact cell adhesion and proliferation [31, 32].

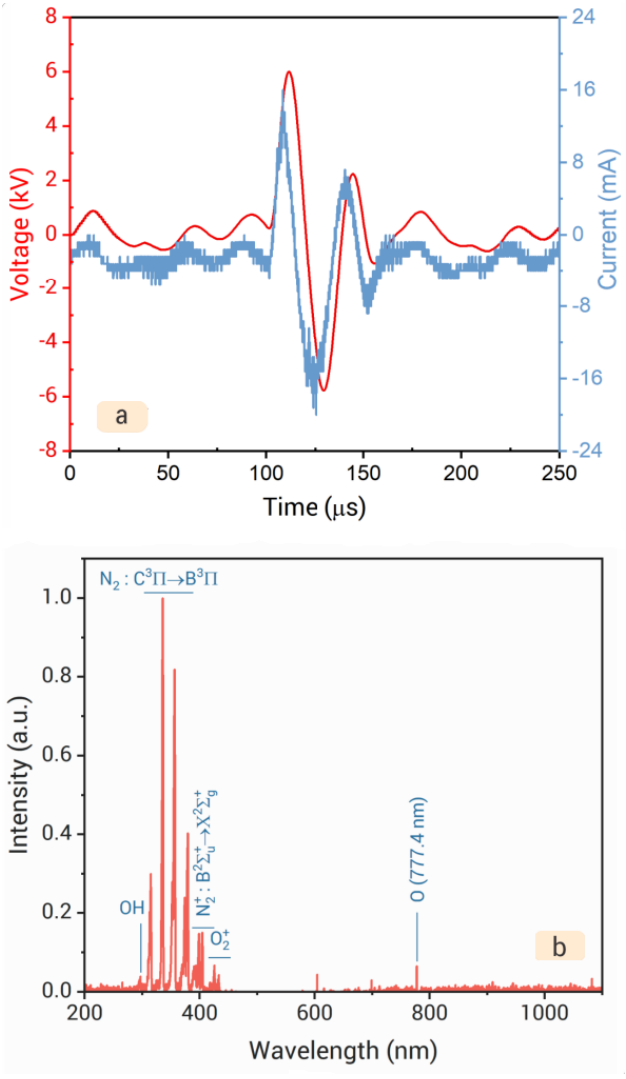

Figure 3. (a) The applied voltage and current waveform to HV electrode, (b) the OES spectrum acquired from DBD plasma.

3.2 Surface chemistry composition

The fibers were subjected to ATR-FTIR analysis, revealing the existence of diverse vibrational modes, as depicted in Fig. 4. The results exhibit distinct peaks, including O-H stretching vibration peak in the range of 3000–3500 cm^{-1}, C-H and CH_2 bending vibrations at 1326 and 1420 cm^{-1}, C-H stretching vibration peaks at 2932 and 2872 cm^{-1}, C≡N stretching vibration peak at 2242 cm^{-1}, double C=O stretching vibration peaks within the range of 1650–1750 cm^{-1}, and C-O stretching vibrations at 1233 and 1093 cm^{-1} [33–36]. The obtained results suggest that plasma treatment induced modifications to the prominent peaks in the ATR-FTIR data. These changes were attributed to the appearance of oxygen- and nitrogen-containing functional groups on the polymer surface [37].

The vibrational modes of C-H bonds can be influenced by the formation of hydrogen bonds with oxygen-containing functional groups, such as hydroxyl, and carbonyl, through air-plasma treatment. This effect has a substantial impact on the C-O and O-H stretching vibrations, resulting in noticeable alterations in the ATR-FTIR spectrum [35]. Moreover, these functional groups can interact with the ester bond (-COO-) through hydrogen bonds or condensation reactions involving the carbonyl group of the ester bond [38]. As a result, the ester bonds from the PAN polymer are integrated into the PVAG layer. This interaction modifies the vibration of the ester bonds, subsequently causing a discernible alteration in either the peak intensity or position observed within the ATR-FTIR spectrum [39–41].

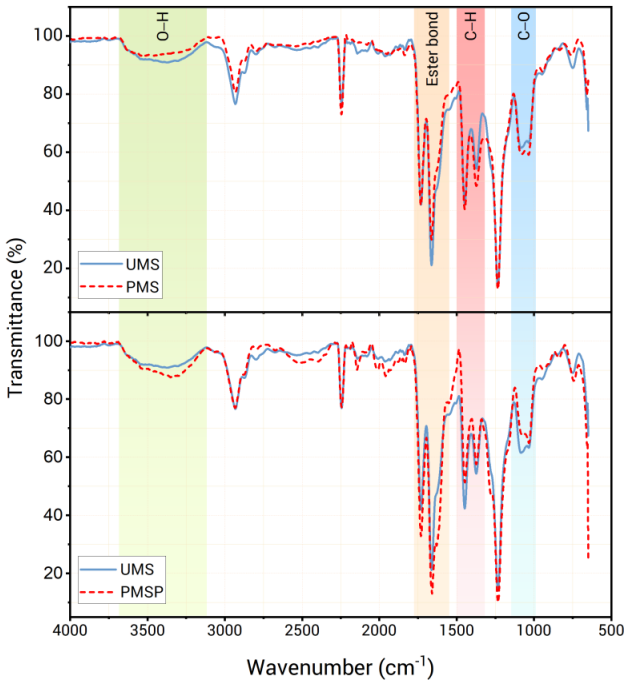

Figure 4. The ATR-FTIR spectra of scaffold fibers.

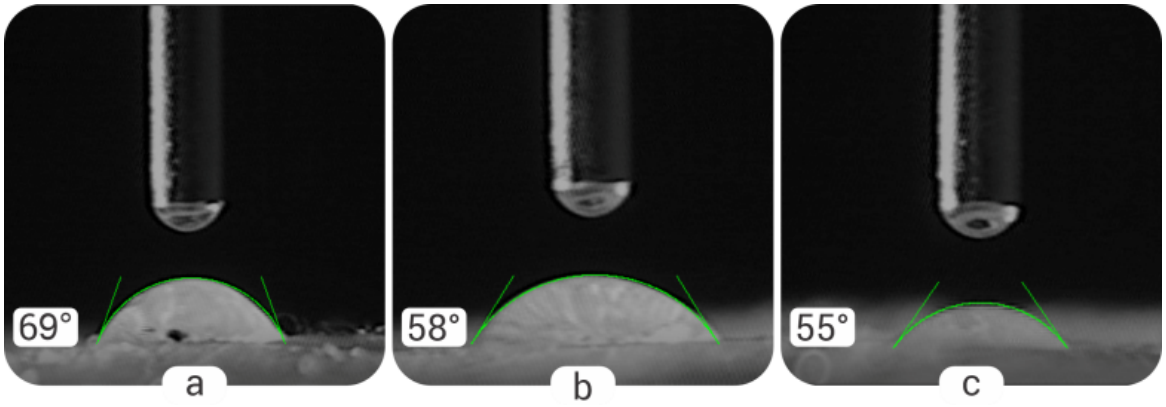

Figure 5. The contact angle of the scaffold surface (a) UMS, (b) PMS, (c) PMSP.

3.3 Contact angle measurement

The hydrophilicity of PAN/PVAG fibers was evaluated under various conditions of plasma surface modification using the drop contact angle method (Fig. 5). The respective contact angles were determined to be 69 degrees for UMS, 58 degrees for PMS, and 55 degrees for PMSP. The plasma treatment applied to the fibers has been demonstrated to enhance the bonding of oxygen molecules to the surfaces of the polymer. This evidence is substantiated by the analysis performed using ATR-FTIR and OES. The results obviously indicate that plasma modification is a viable and effective method for enhancing the surface energy and hydrophilicity of fibers [30, 42]. The dissimilarity in contact angles observed between the PMS and PMSP conditions may be explained by the surface porosity and three-dimensional structure created by the direct plasma treatment applied to the PAN layer under the PMSP condition. The presence of pores enhances the surface area available for water adhesion, which results in reduced contact angles and improved wettability properties [43]. Furthermore, the cross-linked porosity could potentially facilitate capillary action, helping water infiltration into the scaffold material [44].

3.4 Morphology of polymers surface

Fig. 6 presents the SEM images of the scaffold fibers produced through electrospinning before being undergoing plasma treatment. In Fig. 6 a, the electrospun PAN microstructures are shown, highlighting their average thickness and undulating morphology. The PAN fibers exhibit an average thickness of 1.95 μm. The observed wave-like pattern in PAN fibers can be ascribed to the influence of the UV radiation during the electrospinning procedure. When exposed to UV irradiation, the PAN polymer chains undergo simultaneous crosslinking reactions and photodegradation. The crosslinking of the PAN fibers takes place through UV energy absorption, resulting in the formation of covalent bonds between the polymer chains [45]. In addition, photodegradation occurs as a consequence of the cleavage of chemical bonds within the PAN polymer structure, leading to chain fragmentation and molecular weight reduction [46]. These processes are responsible for the wave-like morphology observed in the PAN fibers. The morphology of PVAG fibers is depicted in Fig. 6 b, accompanied by the average thickness measurement. The PVAG fibers during electrospinning can also be affected by UV radiation. The UV energy has the capability to initiate both crosslinking and degradation reactions within the polymer blend, specifically affecting the PVA and gelatin components [46, 47]. This crosslinking enhances the mechanical strength and stability of the electrospun fibers [48].

The application of direct plasma treatment to the PAN fiber layer is a highly effective method for creating surface perforations. The morphology of the PAN fibers that underwent plasma treatment and mean diameter of the generated pores for various treatment durations, ranging from 10 to 60 seconds, are presented in Fig. 7. When the plasma comes into contact with the PAN surface, plasma species bombard it, triggering both chemical reactions and physical sputtering [43, 49]. The plasma reactive species can break chemical bonds within the PAN, while the sputtering effect physically eliminates PAN chains. This combination results in the formation of pores on the PAN surface [50, 51]. Moreover, the resultant etching outcomes, such as the dimensions, configuration, and depth of the perforations, are subject to variation depending on the species generated during the treatment [43]. In addition, the accompanying data offers

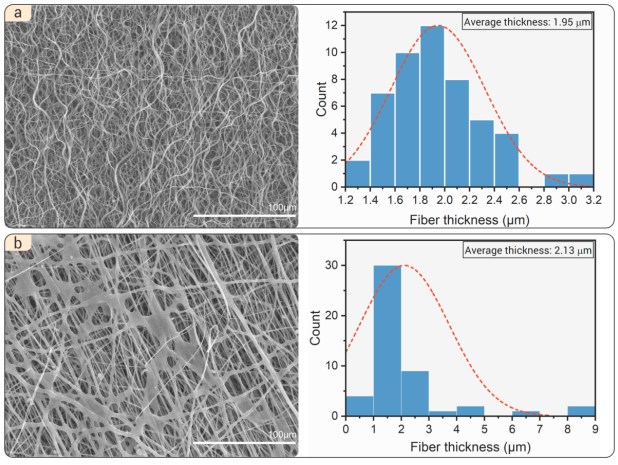

Figure 6. The morphology and the average thicknesses of (a) PAN fibers and (b) PVAG fibers obtained using SEM.

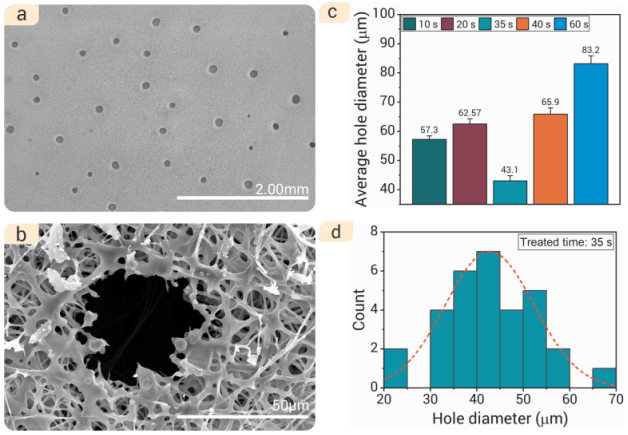

Figure 7. The morphology of PAN fibers after plasma treatment at a scale of (a) 2 mm and (b) 50 μm, as well as the mean diameter of the generated holes at (c) various treated times and (d) 35 seconds.

insights into the average diameter of the pores generated during each specific treatment period. The outcomes reveal that a duration of 35 seconds is the optimal time period for creating pores and channels in the initial layer, resulting in pores with an average diameter of 43 μm. This diameter is suitable for accommodating mouse fibroblast cells, which typically have an average size of 18 μm.

Plasma treatment has the potential to induce crosslinking among PVAG chains, as demonstrated in Fig. 8 a and b. The radicals produced on the surface exhibit the ability to interact with either the polymer chains or the crosslinking agents present in the plasma environment [52]. This facilitates the formation of new covalent bonds [53]. The crosslinking effect results in augmented mechanical strength, enhanced chemical resistance, and improved stability of the PVAG layer [52]. Furthermore, the enhanced stability resulting from crosslinking ensures that the polymer substance maintains its intended characteristics for an extended duration [54, 55]. Fig. 8 c presents the AFM image of the unmodified scaffold, while Fig. 8 d displays the modified scaffold following a 3-minute exposure to air plasma. These images clearly demonstrate that the surface roughness of the scaffold increased as a result of the air plasma treatment.

The analysis of the AFM data yielded significant findings regarding the surface roughness of the fibers. The average surface roughness (Sa) of the unmodified fibers measured 228.9 nm, whereas it increased to 297.9 nm after the plasma modification. Furthermore, the root mean square roughness (Sq) of the unmodified and modified plasma fibers was measured to be 289.8 nm and 362.4 nm, respectively. This data clearly indicates that the plasma treatment alters the scaffold surface morphology, leading to an enhancement in roughness [50, 56]. An increased roughness on the surface of the scaffold provides additional sites for cell attachment, thereby potentially improving cell adhesion and facilitating better integration of the scaffold with the surrounding tissues [30, 43].

Fibroblast cells cultured on fiber surfaces are shown in Fig. 9. The results indicate that plasma-treated fiber scaffolds exhibited cellular attachment and division. In contrast, the non-plasma-treated sample did not exhibit fibroblast cell polarity. Moreover, the observation of cells being drawn into the formed cavities indicates that the scaffold was appropriately designed to accomplish surface modification and three-dimensional cell entrapment [17, 29].

3.5 Fibroblast cells viability and proliferation

The flow cytometry analysis revealed discernible cellular responses within the three scaffold conditions, as demonstrated in Fig. 10. The investigation unveiled noteworthy findings regarding the effects of plasma modification on cell behavior within the scaffold. Without PAN treatment, the necrosis cell proportion on the plasma-modified scaffold increased notably to 21.7%, compared to the plasma-modified scaffold with PAN treatment and the unmodified scaffold ($p < 0.05$).

The direct plasma treatment of the PAN layer results in the

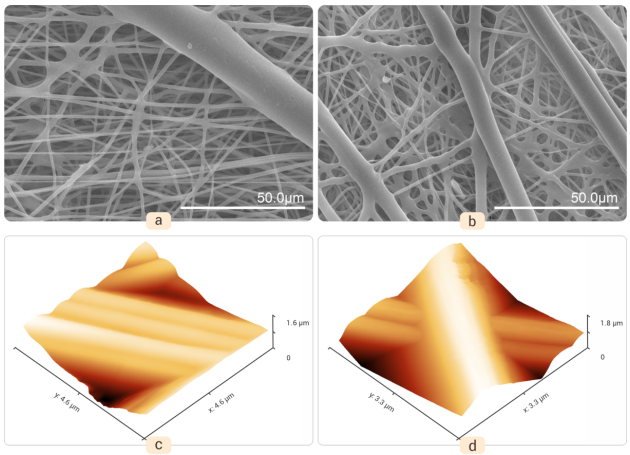

Figure 8. The SEM images of morphology of scaffold surface, (a) unmodified scaffold and (b) plasma modified scaffold, as well as AFM images of PAN/PVAG scaffold surface (c) unmodified and (d) plasma modified.

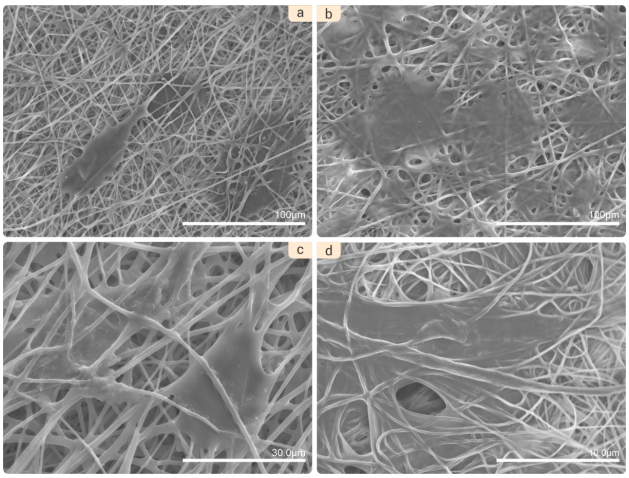

Figure 9. The SEM images of fibroblast cells cultured on scaffold surface, (a) unmodified scaffold, and plasma-modified scaffold at the scale of (b) 100 µm, (c) 30 μm, and (d) 10 μm.

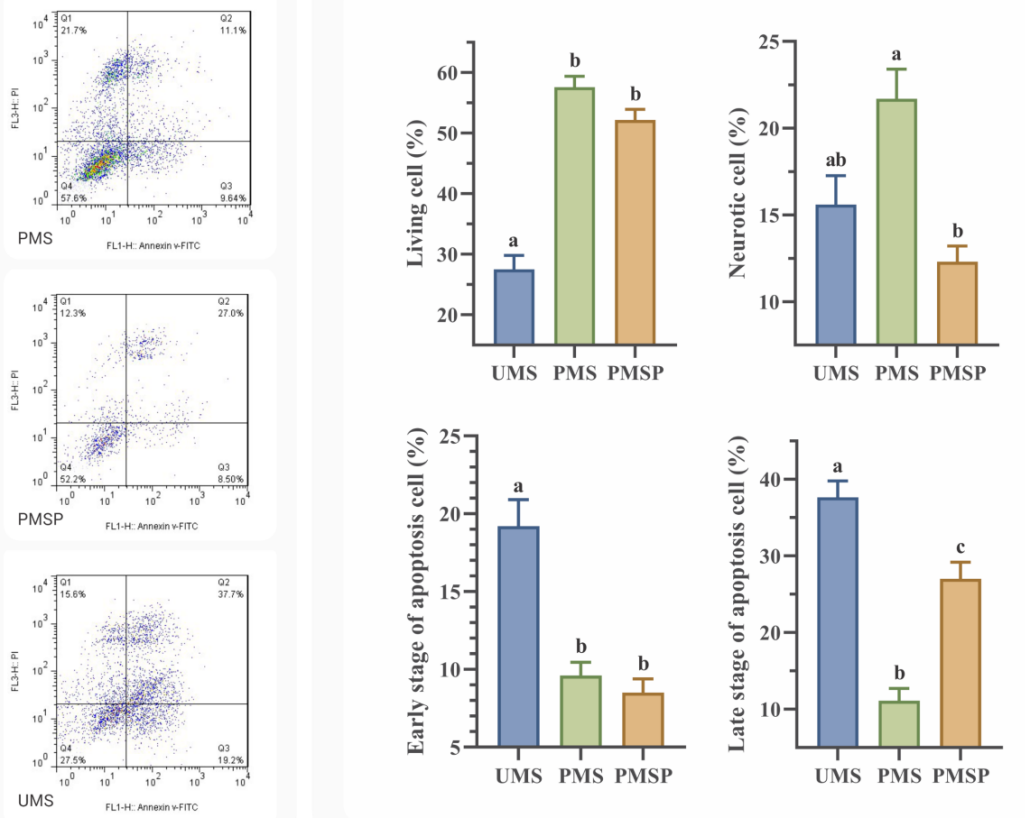

Figure 10. The flow cytometry results of scaffold samples, for which statistical significance was determined as $p < 0.05$.

formation of a porous structure, which offers enhanced capabilities for cell infiltration, nutrient diffusion, and waste removal. The inclusion of plasma-perforated PAN in the scaffold results in enhanced cell viability and reduced necrosis cell formation, as compared to the scaffold lacking this component [57, 58]. The unmodified scaffold displayed a higher percentage of apoptosis cells, with 19.2% in the early-stage and 37.7% in the late stage of apoptosis, compared to the plasma-modified scaffold ($p < 0.05$). In contrast, the proportion of viable cells on the unmodified scaffold (27.5%) decreased significantly compared to both the plasma-treated scaffold ($p < 0.05$). The application of plasma treatment resulted in modifications to the surface charge, hydrophobic characteristics, and surface energy of the polymer scaffolds. Moreover, this treatment method demonstrates the capability to modify the surface chemistry of the polymer scaffold, thereby introducing functional groups such as carbonyl and hydroxyl groups [59]. These functional groups have demonstrated effective interactions with growth factors, ultimately promoting cell adhesion. These factors have been observed to effectively modulate apoptosis pathways and mitigate stress [60, 61].

4. Conclusion

The present research was designed to examine the impact of subjecting PAN/PVA-gelatin polymer scaffolds to DBD plasma in ambient air to mitigate its hydrophobicity limitations and understand the effects of plasma treatment on scaffold synthesis for tissue engineering and cell growth. Furthermore, in order to enhance the properties of the scaffold, an in-situ UV treatment was implemented during the electrospinning process, leading to the formation of a cured layer. The results demonstrated that the plasma treatment had a significant impact on the physiochemical properties of the scaffold surface. The ATR-FTIR analysis indicated the presence of ester bonds of PAN polymer in the PVAG layer as a result of plasma treatment. Furthermore, the application of plasma to modify the PVAG layer facilitated the formation of hydroxyl bonds, consequently enhancing the hydrophilic properties of the scaffold surface. Evaluation of droplet contact angle images demonstrated significantly elevated hydrophilicity on the plasma-modified surface. The SEM analysis revealed the presence of etched pores on the PAN surface, which were attributed to the direct plasma treatment, creating a three-dimensional microenvironment within the scaffold where cells could attach to these cavities. Moreover, when exposed to UV energy, the polymer chains of PAN undergo photodegradation and chain scission, leading to the disruption of the fiber structure and the formation of wave-like patterns. Furthermore, the presence of UV radiation can initiate crosslinking reactions through the generation of free radicals. This process enhances stability of both PAN and PVAG layers and induces structural modifications. This improvement in stability can be attributed to crosslinking, as indicated by the retention of the fibrous architecture following cultivation. The flow cytometry data revealed enhanced biocompatibility of the scaffold, as a substantial proportion of fibroblast cells cultivated on the plasma-treated scaffold exhibited increased cell

viability in comparison to the unmodified control. In conclusion, the results of the present research demonstrate that the plasma modification of PAN/PVA-gelatin scaffold enhances its physio-chemical properties and promotes cellular integration and communication within the scaffold. The aforementioned results make a valuable contribution to the progress of scaffold synthesis in the tissue engineering applications.

Acknowledgment
We would like to express our gratitude to the Shahid Beheshti University Institute Licensing Committee for their approval of all experimental protocols presented in this study. We confirm that all methods employed throughout the research were conducted in strict accordance with the regulations set forth by Shahid Beheshti University. Additionally, we adhered to the ARRIVE guidelines to ensure the highest standards of transparency and reproducibility in reporting our findings.

Ethical Approval
This manuscript does not report on or involve the use of any animal or human data or tissue. So the ethical approval is not applicable.

Authors Contributions
The authors' contributions to this manuscript are as follows: Rahimeh Khavari: Conceptualization, Methodology, Investigation, Validation, Formal Analysis, Writing-Original Draft; Saeed Javadi Anaghizi: Conceptualization, Methodology, Investigation, Validation, Formal Analysis, Writing-Original Draft; Ahmad Khademi: Investigation, Formal Analysis, Visualization, Writing-Original Draft; Mehdi Jahanfar: Supervision, Conceptualization, Methodology, Resources, Writing-Review & Editing; Shirin Farivar: Supervision, Methodology, Resources, Writing-Review & Editing; Hamid Ghomi: Supervision, Methodology, Resources, Writing-Review & Editing

Availability of Data and Materials
All the data generated/analyzed during the study are included in this published article.

Conflict of Interests
The authors declare that they have no known competing financial interests or personal relationships that could have appeared to influence the work reported in this paper.

References

[1] P. Zarrintaj, F. Seidi, M. Y. Azarfam, M. K. Yazdi, A. Erfani, M. Barani, N. P. S. Chauhan, N. Rabiee, T. Kuang, and J. Kucinska-Lipka. "Biopolymer-based composites for tissue engineering applications: A basis for future opportunities.". *Composites Part B: Engineering*, **258**:110701, 2023. DOI: https://doi.org/10.1016/j.compositesb.2023.110701.

[2] M. N. Collins, G. Ren, K. Young, S. Pina, R. L. Reis, and J. M. Oliveira. "Scaffold fabrication technologies and structure/function properties in bone tissue engineering. ". *Advanced Functional Materials*, **31**:2010609, 2021. DOI: https://doi.org/10.1002/adfm.202010609.

[3] H. E. Jazayeri, S.-M. Lee, L. Kuhn, F. Fahimipour, M. Tahriri, and L. Tayebi. "Polymeric scaffolds for dental pulp tissue engineering: A review.". *Dental Materials*, **36**:e47–e58, 2020. DOI: https://doi.org/10.1016/j.dental.2019.11.005.

[4] S. O. Ebhodaghe. "Natural polymeric scaffolds for tissue engineering applications.". *Journal of Biomaterials Science, Polymer Edition*, **32**:2144–2194, 2021. DOI: https://doi.org/10.1080/09205063.2021.1958185.

[5] T. Weigel, G. Schinkel, and A. Lendlein. "Design and preparation of polymeric scaffolds for tissue engineering.". *Expert Review of Medical Devices*, **3**:835–851, 2006. DOI: https://doi.org/10.1586/17434440.3.6.835.

[6] X. He, K. Jia, L. Zheng, Y. Hu, J. Huang, D. Wang, and X. Liu. "Robust polymeric scaffold from 3D soft confinement self-assembly of polycondensation aromatic polymer.". *European Polymer Journal*, **161**:110815, 2021. DOI: https://doi.org/10.1016/j.eurpolymj.2021.110815.

[7] E. S. Place, J. H. George, C. K. Williams, and M. M. Stevens. " Synthetic polymer scaffolds for tissue engineering.". *Chemical Society Reviews*, **38**:1139–1151, 2009. DOI: https://doi.org/10.1039/B811392K.

[8] Y. P. Singh, S. Dasgupta, S. Nayar, and R. Bhaskar. "Optimization of electrospinning

process & parameters for producing defect-free chitosan/polyethylene oxide nanofibers for bone tissue engineering.". *Journal of Biomaterials Science, Polymer Edition*, **31**:781–803, 2020. DOI: https://doi.org/10.1080/09205063.2020.1718824.

[9] D. Sharma, S. Saha, and B. K. Satapathy. "Recent advances in polymer scaffolds for biomedical applications.". *Journal of Biomaterials Science, Polymer Edition*, **33**:342–408, 2022. DOI: https://doi.org/10.1080/09205063.2021.1989569.

[10] A. M. Al-Dhahebi, J. Ling, S. G. Krishnan, M. Yousefzadeh, N. K. Elumalai, M. S. M. Saheed, S. Ramakrishna, and R. Jose. "Electrospinning research and products: The road and the way forward. ". *Applied Physics Reviews*, **9**, 2022. DOI: https://doi.org/10.1063/5.0077959.

[11] M. Rahmati, D. K. Mills, A. M. Urbanska, M. R. Saeb, J. R. Venugopal, S. Ramakrishna, and M. Mozafari. "Electrospinning for tissue engineering applications. ". *Progress in Materials Science*, **117**:100721, 2021. DOI: https://doi.org/10.1016/j.pmatsci.2020.100721.

[12] F. Zhang and M. W. King. "Biodegradable polymers as the pivotal player in the design of tissue engineering scaffolds.". *Advanced Healthcare Materials*, **9**:1901358, 2020. DOI: https://doi.org/10.1002/adhm.201901358.

[13] A. Lipovka, R. Rodriguez, E. Bolbasov, P. Maryin, S. Tverdokhlebov, and E. Sheremet. "Time-stable wetting effect of plasma-treated biodegradable scaffolds functionalized with graphene oxide.". *Surface and Coatings Technology*, **388**:125560, 2020. DOI: https://doi.org/10.1016/j.surfcoat.2020.125560.

[14] C. Karthik, S. Rajalakshmi, S. Thomas, and V. Thomas. "Intelligent polymeric biomaterials surface driven by plasma processing.". *Current Opinion in Biomedical Engineering*, :100440, 2023. DOI: https://doi.org/10.1016/j.cobme.2022.100440.

[15] R. Ghobeira, P. S. E. Tabaei, R. Morent, and N. De Geyter. "Chemical characterization of plasma-activated polymeric surfaces via XPS analyses: A review.". *Surfaces and Interfaces*, :102087, 2022. DOI: https://doi.org/10.1016/j.surfin.2022.102087.

[16] M. Asadian, K. V. Chan, T. Egghe, Y. Onyshchenko, S. Grande, H. Declercq, P. Cools, R. Morent, and N. De Geyter. "Acrylic acid plasma polymerization and post-plasma ethylene diamine grafting for enhanced bone marrow mesenchymal stem cell behaviour on polycaprolactone nanofibers.". *Applied Surface Science*, **563**:150363, 2021. DOI: https://doi.org/10.1016/j.apsusc.2021.150363.

[17] H.-U. Lee, S.-Y. Park, Y.-H. Kang, S.-Y. Jeong, S.-H. Choi, Y.-Y. Jahng, G.-H. Chung, M.-B. Kim, and C.-R. Cho. "Physicochemical properties and enhanced cellular responses of biocompatible polymeric scaffolds treated with atmospheric pressure plasma using O_2 gas. ". *Materials Science and Engineering: C*, **31**:688–696, 2011. DOI: https://doi.org/10.1016/j.msec.2010.12.012.

[18] M. Asadian, K. V. Chan, M. Norouzi, S. Grande, P. Cools, R. Morent, and N. De Geyter. "Fabrication and plasma modification of nanofibrous tissue engineering scaffolds.". *Nanomaterials*, **10**:119, 2020. DOI: https://doi.org/10.3390/nano10010119.

[19] M. Nitschke, G. Schmack, A. Janke, F. Simon, D. Pleul, and C. Werner. "Low pressure plasma treatment of poly (3-hydroxybutyrate): Toward tailored polymer surfaces for tissue engineering scaffolds. ". *Journal of Biomedical Materials Research: An Official Journal of The Society for Biomaterials, The Japanese Society for Biomaterials, and The Australian Society for Biomaterials and the Korean Society for Biomaterials*, **59**:632–638, 2002. DOI: https://doi.org/10.1002/jbm.1274.

[20] G. H. Ryu, W.-S. Yang, H.-W. Roh, I.-S. Lee, J. K. Kim, G. H. Lee, D. H. Lee, B. J. Park, M. S. Lee, and J. C. Park. "Plasma surface modification of poly (D, L-lactic-co-glycolic acid) (65/35) film for tissue engineering.". *Surface and Coatings Technology*, **193**:60–64, 2005. DOI: https://doi.org/10.1016/j.surfcoat.2004.07.062.

[21] S. Yoshida, K. Hagiwara, T. Hasebe, and A. Hotta. "Surface modification of polymers by plasma treatments for the enhancement of biocompatibility and controlled drug release.". *Surface and Coatings Technology*, **233**:99–107, 2013. DOI: https://doi.org/10.1016/j.surfcoat.2013.02.042.

[22] J. Venugopal, S. Low, A. T. Choon, A. B. Kumar, and S. Ramakrishna. "Electrospun-modified nanofibrous scaffolds for the mineralization of osteoblast cells. ". *Journal of Biomedical Materials Research Part A: An Official Journal of The Society for Biomaterials, The Japanese Society for Biomaterials, and The Australian Society for Biomaterials and the Korean Society for Biomaterials*, **85**:408–417, 2008. DOI: https://doi.org/10.1002/jbm.a.31538.

[23] R. Ghobeira, C. Philips, L. Liefooghe, M. Verdonck, M. Asadian, P. Cools, H. Declercq, W. H. De Vos, N. De Geyter, and R. Morent. "Synergetic effect of electrospun PCL fiber size, orientation and plasma-modified surface chemistry on stem cell behavior. ". *Applied Surface Science*, **485**:204–221, 2019. DOI: https://doi.org/10.1016/j.apsusc.2019.04.109.

[24] M. Gozutok, A. Baitukha, F. Arefi-Khonsari, and H. T. Sasmazel. "Novel thin films deposited on electrospun PCL scaffolds by atmospheric pressure plasma jet for L929 fibroblast cell cultivation.". *Journal of Physics D: Applied Physics*, **49**:474002, 2016. DOI: https://doi.org/10.1088/0022-3727/49/47/474002.

[25] S. Sartori, A. Rechichi, G. Vozzi, M. D'acunto, E. Heine, P. Giusti, and G. Ciardelli. "Surface modification of a synthetic polyurethane by plasma glow discharge: Preparation and characterization of bioactive monolayers.". *Reactive and Functional Polymers*, **68**:809–821, 2008. DOI: https://doi.org/10.1016/j.reactfunctpolym.2007.12.002.

[26] C. Zandén, N. H. Erkenstam, T. Padel, J. Wittgenstein, J. Liu, and H. G. Kuhn. " Stem cell responses to plasma surface modified electrospun polyurethane scaffolds.". *Nanomedicine: Nanotechnology, Biology and Medicine*, **10**:e949–e958, 2014. DOI: https://doi.org/10.1016/j.nano.2014.01.010.

[27] M. H. Ghazimoradi, K. Hasegawa, E. Zolghadr, S. Montazeri, and S. Farivar. "Reprogramming of fibroblast cells to totipotent state by DNA demethylation.". *Scientific Reports*, **13**:1154, 2023. DOI: https://doi.org/10.1038/s41598-023-28457-8.

[28] P. Seyfi, M. Keshavarzi, S. Zahedi, A. Khademi, and H. Ghomi. "Low-temperature argon plasma jet with cascading electrode technique for biological applications.". *Scientific Reports*, **12**:17042, 2022. DOI: https://doi.org/10.1038/s41598-022-21664-9.

[29] S. Zhou, L. Wen, Z. Tian, K. C. Yan, J. Cheng, L. Xia, H. Wang, J. Chu, and G. Zou. "Parameter optimization of O_2/He atmospheric pressure plasma for surface modification of poly (L-lactic) acid oriented fiber membranes: Improving cell adhesion and proliferation. ". *Vacuum*, **182**:109763, 2020. DOI: https://doi.org/10.1016/j.vacuum.2020.109763.

[30] A. Vesel and M. Mozetic. "New developments in surface functionalization of polymers using controlled plasma treatments.". *Journal of Physics D: Applied Physics*, **50**:293001, 2017. DOI: https://doi.org/10.1088/1361-6463/aa748a.

[31] M. J. Sherratt, D. V. Bax, S. S. Chaudhry, N. Hodson, J. R. Lu, P. Saravanapavan, and C. M. Kielty. "Substrate chemistry influences the morphology and biological function of adsorbed extracellular matrix assemblies.". *Biomaterials*, **26**:7192–7206, 2005. DOI: https://doi.org/10.1016/j.biomaterials.2005.05.010.

[32] R. Tzoneva, N. Faucheux, and T. Groth. "Wettability of substrata controls cell–substrate and cell–cell adhesions.". *Biochimica et Biophysica Acta (BBA)-General Subjects*, **1770**:1538–1547, 2007. DOI: https://doi.org/10.1016/j.bbagen.2007.07.008.

[33] R. Damayanti, Z. Alfian, and M. Zulfajri. "Biosynthesis of silver nanoparticles loaded PVA/gelatin nanocomposite films and their antimicrobial activities.". *Inorganic Chemistry Communications*, **144**:109948, 2022. DOI: https://doi.org/10.1016/j.inoche.2022.109948.

[34] H. Xi, D. Chen, L. Lv, P. Zhong, Z. Lin, J. Chang, H. Wang, B. Wang, X. Ma, and C. Zhang. "High performance transient organic solar cells on biodegradable polyvinyl alcohol composite substrates. ". *RSC advances*, **7**:52930–52937, 2017. DOI: https://doi.org/10.1039/C7RA11191F.

[35] N. Ojah, D. Saikia, D. Gogoi, P. Baishya, G. A. Ahmed, A. Ramteke, and A. J. Choudhury. "Surface modification of core-shell silk/PVA nanofibers by oxygen dielectric barrier discharge plasma: Studies of physico-chemical properties and drug release behavior. ". *Applied Surface Science*, **475**:219–229, 2019. DOI: https://doi.org/10.1016/j.apsusc.2018.12.270.

[36] M. Tüfekci, S. G. Durak, I. Pir, T. O. Acar, G. T. Demirkol, and N. Tüfekci. "Manufacturing, characterisation and mechanical analysis of polyacrylonitrile membranes.". *Polymers*, **12**:2378, 2020. DOI: https://doi.org/10.3390/polym12102378.

[37] V. S. Rosa, T. dos Santos Mendonça, R. H. Mendonça, R. A. Simao, and D. C. Bastos. "Application of atmospheric-air plasma on polyhydroxybutirate solution–evaluation of promoted changes on the casted film surface and nanoparticles production.". *Macromolecular Symposia*, **406**:2200041, 2022. DOI: https://doi.org/10.1002/masy.202200041.

[38] Y. Kang, K. Ahn, S. Jeong, J. Bae, J. Jin, H. Kim, S. Hong, and C. Cho. "Effect of plasma treatment on surface chemical-bonding states and electrical properties of polyacrylonitrile nanofibers.". *Thin Solid Films*, **519**:7090–7094, 2011. DOI: https://doi.org/10.1016/j.tsf.2011.04.056.

[39] X. Fu, M. J. Jenkins, G. Sun, I. Bertoti, and H. Dong. "Characterization of active screen plasma modified polyurethane surfaces. ". *Surface and Coatings Technology*, **206**:4799–4807, 2012. DOI: https://doi.org/10.1016/j.surfcoat.2012.04.051.

[40] B. Dashtbozorg, X. Tao, and H. Dong. "Active-screen plasma surface multi-functionalisation of biopolymers and carbon-based materials–An overview.". *Surface and Coatings Technology*, **442**:128188, 2022. DOI: https://doi.org/10.1016/j.surfcoat.2022.128188.

[41] Y. Liang, X. Li, D. Semitekolos, C. A. Charitidis, and H. Dong. "Enhanced properties of PAN-derived carbon fibres and resulting composites by active screen plasma surface functionalisation.". *Plasma Processes and Polymers*, **17**:1900252, 2020. DOI: https://doi.org/10.1002/ppap.201900252.

[42] C.-Y. Wang, M. Schön, T. Horn, M. Facklam, R. Dahlmann, C. Hopmann, and G.-J. He. "Usage of atmosphere pressure plasma for rapid polyethylene functionalisation exhibiting only minor ageing.". *European Polymer Journal*, **181**:111669, 2022. DOI: https://doi.org/10.1016/j.eurpolymj.2022.111669.

[43] L. T. Phan, S. M. Yoon, and M.-W. Moon. "Plasma-based nanostructuring of polymers: A review.". *Polymers*, **9**:417, 2017. DOI: https://doi.org/10.3390/polym9090417.

[44] L. Vikingsson, B. Claessens, J. A. Gómez-Tejedor, G. G. Ferrer, , and J. G. Ribelles. "Relationship between micro-porosity, water permeability and mechanical behavior in scaffolds for cartilage engineering.". *Journal of the Mechanical Behavior of Biomedical Materials*, **48**:60–69, 2015. DOI: https://doi.org/10.1016/j.jmbbm.2015.03.021.

[45] B. Sieredzinska, Q. Zhang, K. J. van den Berg, J. Flapper, and B. L. Feringa. "Photo-crosslinking polymers by dynamic covalent disulfide bonds.". *Chemical Communications*, **57**:9838–9841, 2021. DOI: https://doi.org/10.1039/D1CC03648C.

[46] E. Yousif and R. Haddad. "Photodegradation and photostabilization of polymers, especially polystyrene. ". *SpringerPlus*, **2**:1–32, 2013. DOI: https://doi.org/10.1186/2193-1801-2-398.

[47] A. Michele, D. Luft, G. E. Tovar, and A. Southan. "Photo-crosslinking and surface-attachment of polyvinyl alcohol nanocoatings by C, H insertion to customize their swelling behavior and stability in polar media.". *Polymer Chemistry*, **13**:4273–4283, 2022. DOI: https://doi.org/10.1039/D2PY00443G.

[48] D. Choi, M. H. Khan, and J. Jung. "Crosslinking of PVA/alginate carriers by glutaraldehyde with improved mechanical strength and enhanced inhibition of deammonification sludge. ". *International Biodeterioration & Biodegradation*, **145**:104788, 2019. DOI: https://doi.org/10.1016/j.ibiod.2019.104788.

[49] O. Neděla, P. Slepička, and V. Švorčík. "Surface modification of polymer substrates for biomedical applications. ". *Materials*, **10**:1115, 2017. DOI: https://doi.org/10.3390/ma10101115.

[50] F. Palumbo, C. Lo Porto, and P. Favia. "Plasma nano-texturing of polymers for wettability control: why, what and how.". *Coatings*, **9**:640, 2019. DOI: https://doi.org/10.3390/coatings9100640.

[51] K. Fricke, H. Steffen, T. Von Woedtke, K. Schröder, and K. D. Weltmann. "High rate etching of polymers by means of an atmospheric pressure plasma jet.". *Plasma Processes and Polymers*, **8**:51–58, 2011. DOI: https://doi.org/10.1002/ppap.201000093.

[52] D. Hegemann and S. Gaiser. "Plasma surface engineering for manmade soft materials: A review. ". *Journal of Physics D: Applied Physics*, **55**:173002, 2021. DOI: https://doi.org/10.1088/1361-6463/ac4539.

[53] M. Hamdi, M. N. Saleh, and J. A. Poulis. "Improving the adhesion strength of polymers: effect of surface treatments. ". *Journal of Adhesion Science and Technology*, **34**:1853–1870, 2020. DOI: https://doi.org/10.1080/01694243.2020.1732750.

[54] H. B. Baniya, R. P. Guragain, and D. P. Subedi. "Cold atmospheric pressure plasma technology for modifying polymers to enhance adhesion: A critical review.". *Progress in Adhesion and Adhesives*, **6**:841–879, 2021. DOI: https://doi.org/10.1002/9781119846703.ch19.

[55] G. S. Oehrlein, R. J. Phaneuf, and D. B. Graves. "Plasma-polymer interactions: A review of progress in understanding polymer resist mask durability during plasma etching for nanoscale fabrication. ". *Journal of Vacuum Science & Technology B, Nanotechnology and Microelectronics: Materials, Processing, Measurement, and Phenomena*, **29**:010801, 2011. DOI: https://doi.org/10.1116/1.3532949.

[56] J.-P. Booth, M. Mozetič, A. Nikiforov, and C. Oehr. "Foundations of plasma surface functionalization of polymers for industrial and biological applications. ". *Plasma Sources Science and Technology*, **31**: 103001, 2022. DOI: https://doi.org/10.1088/1361-6595/ac70f9.

[57] D. Jeyachandran and M. Cerruti. "Glass, ceramic, polymeric and composite scaffolds with multi-scale porosity for bone tissue engineering.". *Advanced Engineering Materials*, , 2023. DOI: https://doi.org/10.1002/adem.202201743.

[58] F. Intranuovo, R. Gristina, F. Brun, S. Mohammadi, G. Ceccone, E. Sardella, F. Rossi, G. Tromba, and P. Favia. "Plasma modification of PCL porous scaffolds fabricated by solvent-casting/particulate-leaching for tissue engineering. ". *Plasma Processes and Polymers*, **11**:184–195, 2014. DOI: https://doi.org/10.1002/ppap.201300149.

[59] S. Sedaghat, V. Kasi, S. Nejati, A. Krishnakumar, and R. Rahimi. "Improved performance of printed electrochemical sensors via cold atmospheric plasma surface modification. ". *Journal of Materials Chemistry C*, **10**:10562–10573, 2022. DOI: https://doi.org/10.1039/D2TC00905F.

[60] S. Miroshnichenko, V. Timofeeva, E. Permyakova, S. Ershov, P. Kiryukhantsev-Korneev, E. Dvořaková, D. V. Shtansky, L. Zajíčková, A. Solovieva, and A. Manakhov. "Plasma-coated polycaprolactone nanofibers with covalently bonded platelet-rich plasma enhance adhesion and growth of human fibroblasts. ". *Nanomaterials*, **9**:637, 2019. DOI: https://doi.org/10.3390/nano9040637.

[61] Y. Xie, T. Sproule, Y. Li, H. Powell, J. J. Lannutti, and D. A. Kniss. "Nanoscale modifications of PET polymer surfaces via oxygen-plasma discharge yield minimal changes in attachment and growth of mammalian epithelial and mesenchymal cells in vitro.". *Journal of Biomedical Materials Research: An Official Journal of The Society for Biomaterials, The Japanese Society for Biomaterials, and The Australian Society for Biomaterials and the Korean Society for Biomaterials*, **61**:234–245, 2002. DOI: https://doi.org/10.1002/jbm.10141.